Int. J. Electrochem. Sci., 7 **(2012)** 8420 - 8435

International Journal of
ELECTROCHEMICAL
SCIENCE
www.electrochemsci.org

Proton and Oxygen Ionic Conductivity of Doped Ceria-Carbonate Composite by Modified Wagner Polarization

Liangdong Fan[1,2,§], *Guoquan Zhang*[1,§], *Mingming Chen*[1,*], *Chengyang Wang*[1], *Jing Di*[1], *Bin Zhu*[2,*]

[1] Key Laboratory for Green Chemical Technology of Ministry of Education, School of Chemical Engineering and Technology, Tianjin University, Tianjin 300072, PR China
[2] Department of Energy Technology, Royal Institute of Technology, SE-100 44 Stockholm, Sweden
[§]both authors contribute equally to this article
[*]E-mail: chmm@tju.edu.cn; binzhu@kth.se

Received: 6 June 2012 / *Accepted:* 15 July 2012 / *Published:* 1 September 2012

The impressive ionic conductivity and tunable conduction behaviors have made the ceria-carbonate composite an attractive electrolyte for low temperature ceramic fuel cells. However, the conduction mechanism is not yet well studied. In the present study, both proton and oxygen ion conductivity as well as the transport properties of samaria-doped ceria/ sodium-lithium-carbonate (denoted as SDCLN) composite are investigated by the fuel cell study and the modified Hebb-Wagner polarization measurements. The multi-ionic polarization behaviors and the transfer processes in composite electrolyte under external electrical field are analyzed. A maximum power density of 780 mW cm^{-2} and a calculated total ion (proton and oxygen ion) conductivity of 0.153 S cm^{-1} are obtained under H_2/ air condition at 550 ^oC. The Wagner DC polarization measurements show that the proton conduction dominates the total ionic conductivity. A synergistic effect exists between the charge carriers in the doped ceria-carbonate composite system. An ideal interfacial conduction model is also proposed based on the obtained results.

Keywords: Solid oxide or ceramic fuel cell; Ceria-carbonate composite electrolyte; Proton and oxygen ion conductivity; Wager polarization; Synergistic effect

1. INTRODUCTION

In recent years, Ceria-based composite materials have been extensively studied as the electrolyte for low temperature solid oxide fuel cells (SOFCs) or ceramic fuel cells [1-22]. It has been demonstrated with many advantages over single-phase electrolytes: i) higher conductivity of 10^{-2} -10^{-1} S cm^{-1} at 500 - 600 ^oC; ii) restraint partial reduction of Ce^{4+} to Ce^{3+} and iii) improved mechanical properties. These composites have also been successfully proved with other advanced applications [23-

27], such as direct carbon fuel cells [23,24] and CO_2 separation membrane [25,26]. All of these make SDC-salts composites as the star materials in energy and environmental related field.

Except the high ionic conductivity as the electrolyte for SOFC, the tunable ion conductive properties also attracted growing attention in the past years. In order to better understand the ionic transport process in the SDC-carbonate composite, several techniques have been presented by different research groups [2,5-7,9,11,12,25,28-31]. In the earlier study, we have reported that the ceria-salt composite system was a mixed oxygen ion and proton conductor [1,2,32]. Following with this work, Huang et al. [6,28] proved this by experimental observation: water was produced at both electrode sides. Moreover, their further study showed that the SDCLN system could be a pure proton conductor with a composition optimization [7]. Thereafter, W. Zhu and his co-workers [5] found that the carbonate ion was the dominant charge and co-existed with proton and oxygen ion conductions. They also found that electronic conductivity was negligible as compared to that of the ions based on the concentration cells at different gas atmosphere. The conductive properties of SDC-carbonate were also examined by Boden et al. [29] using advanced complex impedance spectroscopy. However, they were not able to come up with any specific findings. The contributions of proton and oxygen ion conduction in SDC-$(Li/Na)_2CO_3$ were also studied by Di et al. [12] using the water concentration cells; and the oxygen ionic conduction were shown to dominate the whole ionic behaviors. While X. Wang [30] presented that the proton conductivity of SDC-Na_2CO_3 was 1-2 orders of magnitude higher than the oxygen ion conductivity in the temperature range of 200-600 °C using the four-probe DC technique. More recently, an interesting work has been reported about SDCLN composite which was demonstrated to a ternary ionic conductor, O^{2-}, H^+ and CO_3^{2-}. Besides, the introduction of CO_2 to cathode gas at fuel cell condition could improve the fuel cell performance [9,11,25]. The multi-ionic conduction of composite electrolyte was quantified by careful reaction production analysis [31].

Based on the above discussions and the fallouts, we can find the complexity nature in the ceria-slat two-phase composite systems. Also, it should be noticed that the contributions of multi-ionic conductivities in these materials are multi-parameters effect, such as the electrolyte composition, the microstructures, particle size & distribution and morphology, temperature and most important the applied in-situ atmospheres [33]. Moreover, for a multi-ion conductive system, coexisting blocking and non-blocking mobile ions, and in particular integrated with an open system in which both the intrinsic and extrinsic ions are available, there are, however, current not any analysis techniques and experimental methods to depict such a complex system. While the investigation of the ionic conduction behaviors and mechanism for such a complex system needs one general but valid methodology considering that the experimental and technological exploitation of these materials is apparently moving faster than the understanding of their performance. Therefore, ionic polarization process in doped ceria-carbonate is still an open field to be discussed and needs more comprehensive studies.

Hebb–Wagner polarization is a widely used experimental technique for separating the ionic and electronic conductivity of a mixed conductor [34-36]. Through an analysis of the steady state *I-V* curves, the desirable partial conductivity can be obtained. Although the method has been broadly used in high temperature electrochemical device [37-40], majorly on the mixed ionic and electronic conductive doped ceria electrolyte [41,42], the application in the ceria-salt composite system is seldom

reported [10,21,30]. Therefore, in this work, we used a modified Wagner polarization approach to study the ionic transport behavior in SDCLN composite electrolyte. The traditional Wagner polarization was generally used to separate the ionic conductivity from the electronic conductivity by an ionic blocking electrode. Yet, hereby, ions other than the source ions are separated, because only the source ions can steady-state transport under the external electrical field. In other words, only the proton transport in hydrogen atmosphere or the O^{2-} migration in oxygen in the SDC-carbonate composite electrolyte would be analyzed. It is well recognized that the conductions of H^+ and O^{2-} are the key issues in the ceria-based composite electrolyte based fuel cell and other applications [23,24,27].

2. EXPERIMENTAL

2.1. Preparation of composite electrolyte

$Ce_{0.8}Sm_{0.2}O_{1.9}$ (SDC) powder was prepared by a co-precipitation process. Precursory solution was obtained by dissolving of $Ce(NO_3)_3 \cdot 6H_2O$ and $Sm(NO_3)_3 \cdot 6H_2O$ in water. A white precipitant was obtained by dripping the precursory solution to the sodium carbonate solution until a near-neutral pH of 8.0. After being filtrated and washed with deionized water and pure ethanol, the precipitant was dried and calcined at 700 ^oC for 2 h. The resulted SDC was then blended with binary carbonate with a weight ratio of SDC to carbonate to be 4:1. The molar ratio of Li_2CO_3 to Na_2CO_3 is 2:1. The composite was again heated at 680 ^oC for 40 min and quenched in air. The resultants were ground for further use.

2.2. Single cells fabrication

Three types of single cells were fabricated with SDCLN electrolyte supported configurations. The total pellet thicknesses are 1 mm. One is for fuel cell measurement with Ni anode and lithiated NiO cathode. The detailed fuel cell preparation can be found in our previous publications [12,16]. The electrolyte thickness for this study is around 600 μm. The other one is the symmetrical cells for electrical conductivity characterizations. The electrodes are either NiO or lithiated NiO for reducing and oxidation atmosphere, respectively. They are mixed with SDCLN in an equal volume. After being co-pressed at 300 MPa with electrolyte layer, the surface of the electrode is covered with silver paste as the current collector. The last one is the electrolyte pellet only with silver paste. All the pellets have a diameter of 13 mm and are sintered at 600 ^oC for 30 min to achieve a good mechanical strength and to activate the interface between electrolyte and electrode.

2.3. Electrochemical measurements

Electrical properties were first measured using the fuel cell *I-V* polarization characteristics. The *I-V* polarization curves were recorded by a fuel cell tester (SM-102, Tianjin Sanmu Cop. China). The humidified hydrogen (3 Vol % H_2O) and air are used fuel and oxidation, respectively.

Wagner DC polarizations were measured in air and in the pure hydrogen atmosphere, respectively. A constant current of 0.1 A was applied by regulated power supply (Labornetzgerät/ Lab

515. The resulted voltage was recorded with time. All the samples are sealed with silver glue. The gas velocity of flow, 100 ml min^{-1}, was controlled by a precise gas flow-meter. The scheme for the electrical conductivity measurement is depicted in Fig. 1. To establish a definite source ionic distribution in the sample, the samples were put in applied gas atmospheres for 2 h prior to connecting to the regulated power supply.

The samples were fixed on the sample holder and horizontally put into a tubular furnace [23]. The temperature of the furnace was controlled by a Eutherm temperature controller and the pellet temperature was measured using a Platinum thermocouple close to the pellet. Mostly, the measurements were carried out between 400 - 600 °C. All the data are normalized by the thickness of the electrolyte to calculate the electrical conductivity.

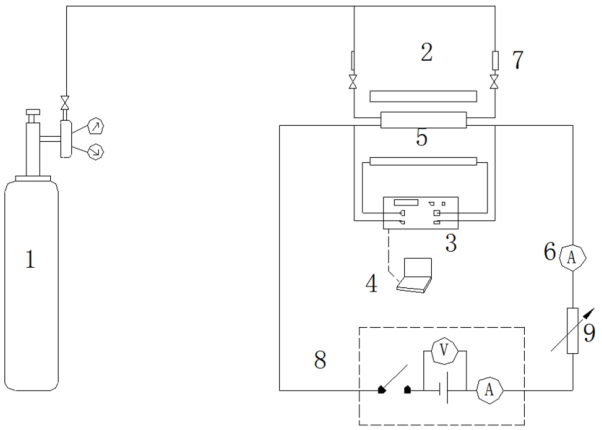

1. Pure hydrogen/air bottle; 2. Electrical furnace; 3. Temperature controller and data; 4. Data processor; 5. Pellet sample; 6. Inspection ammeter; 7. Precious gas flow-meter; 8. Regulated power supply and 9. Resistance

Figure 1. Schematic of electrochemical properties measurement for composite electrolyte

3. RESULTS AND DISCUSSION

3.1. DC conductivity under fuel cell operation

The complex AC impedance measurement is a common way to acquire material conductivity. However, the AC conductivity reflects contributions from all mobile charge carriers:

$$\sigma = \Sigma\sigma_i$$

Where i represents mobile charge carrier in the SDC-carbonate composite electrolyte. The mobile charge carriers are Li+, Na^+, CO_3^{2-} and O^{2-}. When it is treated in fuel cell or hydrogen or humidified atmospheres, H^+ will be introduced additionally. Therefore, the specific charge carrier contribution is difficult to figure out. More important, the ionic contribution to fuel cell performance cannot be identified. This aspect may explain the study results “no mechanism for ionic transport can

be concluded" by Bodén et al [29] on the conductivities of the SDC-carbonate composite system in reducing and oxidizing atmospheres by complex electrochemical impedance spectroscopy.

In addition, the SDC-carbonate composite with 20 wt. % of carbonate is used in this study because of the sufficient percolation paths to contribute ionic mobility and conductivity values as well as the best performance in fuel cells as reported in the literature [6,28].

Fuel cell characterizations were suggested as a useful tool to in-situ analyse the conductivity of the electrolyte material [43]. In some cases, the conductivity derived from the fuel cell study can closely represent the material's electrical conductivity, especially when the materials' non-stoichiometry in specific environments and the system with multi-mobile ion conductions were considered. According to the literature [43], through a direct measurement of *I-V* characteristics, the electrolyte area resistance (*R*) can be determined after subtraction of the influence of the electrodes and electrolyte/electrode interfaces. The conductivity (σ) of electrolyte can be calculated by the following equation:

$$\sigma = L/R$$

In which *L* is the effective thickness of electrolyte layer.

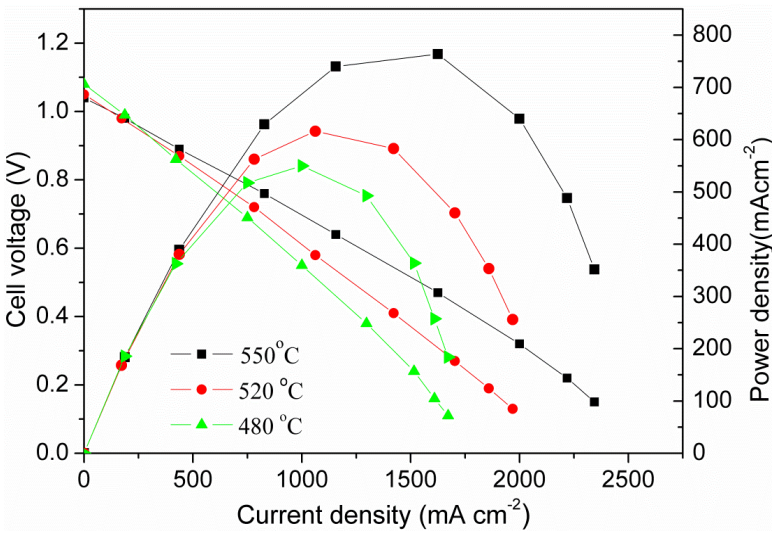

Figure 2. I-V and I-P characteristics of fuel cells with SDC-20 wt. % $LiNaCO_3$ composite electrolyte supported configuration at various temperatures

Fig. 2 illustrates the *I-V* and *I-P* characteristics for the H_2/air fuel cell with SDC-20 wt. % carbonate composite electrolyte at 480 °C, 520 °C and 550 °C, respectively. The open-circuit voltages (OCVs) reach 1.04 V at 550 °C and 1.08 V at 480 °C, which is close to the theoretical values by the Nernst equation, pointing out the SDC-carbonate composite electrolyte layer possesses acceptable density. It also shows that the n-type electronic conduction of doped ceria has been sufficiently suppressed in composite electrolyte. Also, an excellent power density of 780 mW cm^{-2} has been achieved under the current density of 1500 mA cm^{-2} at 550 °C. The total ionic conductivities of

SDCLN in the fuel cell environment are 0.153 and 0.100 S cm^{-1} at 550 ^oC and 480 ^oC, respectively. The conductivity value is much higher than those of single phase cubic fluorite ionic conductors at the same temperature, such as SDC (700 ^oC, 0.1 S cm^{-1}) and stabilized Zirconia (1000 ^oC, 0.1 S cm^{-1}) [44]. The high ionic conductivity can also explain the excellent electrochemical performance at the reduced temperatures.

3.2. DC conductivity by Wagner polarization

As demonstrated earlier, the electronic conductivity of doped ceria has been effectively depressed in the SDCLN, thus the fuel cells can well reach an OCV above 1.0 V compared to the pure SDC electrolyte fuel cell, only less than 0.95 V obtained above 450 ^oC [45]. Also the electronic conductivity of composite electrolyte has been checked by Wei Zhu et al. [5] with a Hebb-Wagner's ion-blocking cell. They found that the electronic conductivity of SDC-carbonate was about 10^{-4} S cm^{-1} at 500 - 550 ^oC, about two to three orders of magnitude lower than the total conductivity. Therefore, the electronic conductivity is negligible and the SDCLN composite system can be considered as a pure ionic conductor.

As discussed above, the SDC-carbonate fuel cell is a multi-ion conductive system, containing Li^+, Na^+, CO_3^{2-}, O^{2-} and H^+ (with humidified gas or H_2 and fuel cell environment). It has been found that only H^+, O^{2-} and H^+/O^{2-} contribute respectively to the valuable electrochemical properties in hydrogen gas, air (oxygen) and fuel cell condition. In the last several years, extensive works have been carried out and have demonstrated that the H^+ and O^{2-} transport in SDCLN composite. However, few are concerned on direct characterizing and separating these ions transportation properties [12,30,31]. Therefore, a general but valid approach needs to be developed which can better uphold the experimental system and show new ways for the research.

In classic Hebb and Wagner polarization measurements, the electronic conductivity of the cuprous halides has been deduced from current density-potential curves with the cell configuration:

Cu/ CuX/ graphite

Where 'X' denotes Cl, Br or I. Under steady-state conditions, no ionic current flows with the ionic blocked graphite, only the electrons or holes can transport [34-36]. In this work, however, with the assumption of negligible electronic conduction in SDCLN composite, the aimed ions, proton or oxygen ionic conductivity are studied by the modified Wagner polarization under the oxidation or reduction atmosphere, respectively. Two different cell configurations are used to figure out the electrode polarization effect on the ionic conductivity:

Cell A: Ag (paste)/ mixed electrode/ electrolyte/ mixed electrode/ Ag (paste)

Cell B: Ag (paste)/ electrolyte/ Ag (paste)

The mixed electrodes are Ni/SDC-carbonate and lithiated NiO/SDC-carbonate, respectively, which are the commonly used as anode and cathode electrode materials for SDCLN composite electrolyte. The works has been carried out both in hydrogen and oxygen atmospheres, respectively.

3.2.1 Proton conductivity

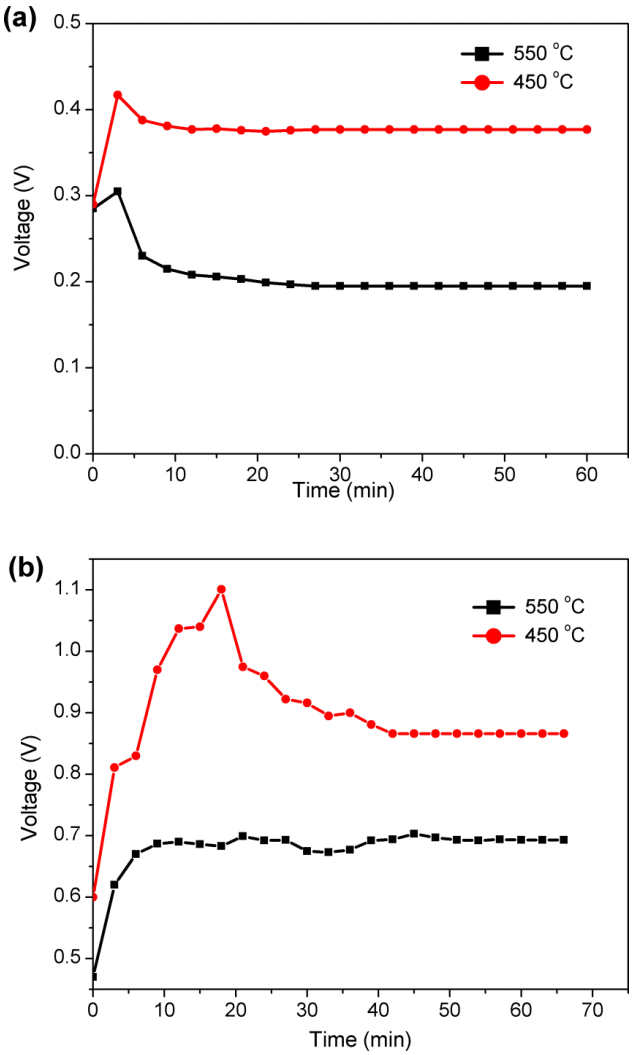

Figure 3. The Wagner DC polarization curve of electrolyte pellets under H_2 ambience and 0.1 A invariable current. (a) cell A and (b) cell B

The proton conduction in the high temperature fuel cell has attracted considerable attention in recent years because the proton transfer has much lower activation energy than the oxygen ionic conduction [46]. Especially, the proton conductor as the electrolyte for fuel cells has a higher theoretical efficiency compared to its competitor oxygen ionic conductor [47]. However, the development of high temperature devices based on proton conductors is hindered by the lower proton conductivity, mismatched superior performance electrode materials as well as the tradeoff effect between electrical conductivity and chemical stability [48,49]. The lower proton conductivity is probably restricted by the structural ionic conduction; the large grain boundary resistance leads to low total conductivity. In SDCLN system, the addition of carbonate not only effectively improves the oxygen ionic conductivity, but also introduces the extrinsic proton transportation, thereby, with much improved electrochemical performance [6,7,13]. Therefore, the proton conductivity in the composite electrolyte is worth and interesting to investigate.

Fig. 3 shows the polarization voltages as function of times in hydrogen atmosphere with two different cell configurations. Once the current is applied, H^+ migrates initially from one side to another. The electrochemical reactions occurring at the electrodes are:

Anode: $H_2 - 2e^- \rightarrow 2H^+$

Cathode: $2H^+ + 2e^- \rightarrow H_2$

As can be seen from Fig. 3, the voltage vs. time curves can be divided into three stages both for cell A and cell B, which may reflect different ionic polarization steps. At the beginning of the measurement, the voltage increases significantly with time, then it reduces gradually and reaches a platform. The voltage final keeps a constant value until the end of the testing.

Since the proton conduction is an extrinsic ionic behavior of SDCLN composite; there is no original proton conduction inside composite electrolyte. While the other ions, like Na^+, Li^+ and CO_3^{2-} and O^{2-}, are homogeneously dispersed within the electrolyte before constant current is applied. They will also mobile under the electrical field. These non-sources or blocked ions move to and accumulate at the electrode/electrolyte interface, to form a voltage that will against the existed external electric field. In order to keep a constant current output which can be only supported by the sources ions, proton in this case, the voltage therefore has to increase. Further going with the applied time, the protons are continuously introduced into the electrolyte and move to another side. The migration of other non-source cations and anions finally reaches a balance distribution according to the polarization provided by the supplied electrical field. Simultaneously, the accumulated blocking ions stay in the other electrode/ electrolyte interface, behaving as a double layer capacitor. With the time increases, the proton conduction path in SDCLN composite turns to be more and more successive. Moreover, the interfaces between electrodes and electrolyte are progressively activated. The polarization deduced proton transport resistance hence reduces. Thus the applied voltage correspondingly declines. After a full relaxation, a balanced concentration of ions is formed in the electrolyte, and electrode/electrolyte interfaces become connected gradually, assuming that and proton conductivity is approaching a constant. At last, H^+ can transport continuously at a steady-stable plateau.

It also can be seen from Fig. 3, with the increase of operational temperature from 450 ^oC to 550 ^oC, the voltage declines significantly, suggesting that the proton transport in the SDCLN composite electrolyte is a thermal active process, similar to those of widely investigated high temperature proton conductors [50,51], such as $BaCe_{1-x}Y_xO_{3-\delta}$ and $BaZr_{1-x}Y_xO_{3-\delta}$. However, their transport route is absolutely different since the proton transports in doped ceria and carbonate, respectively, are negligible at the same condition compared to other charge carriers. It has some similarities to the proton conduction in nanoscale fluorite-structured oxides at low temperature and humidified atmosphere, where the surface or grain boundary proton migration is proposed [52-54], but it should be noted that, in nanoscale oxide, the conductivity reduces quickly with temperature increase. About the proton conduction mechanism, it still not yet forms a consensus, but the interfacial conduction mechanism may come to a conclusion and being majorly accepted [12,16,55,56].

In addition, both cells (A and B) follow the same ionic polarization process. However, voltage responses of various electrodes exhibit clear discrepancies. The cell with oxide mixed electrodes shows a much lower resulted voltage than the cell with Ag electrodes. Typically, the voltage of the cell with Ni/SDCLN electrode is 0.38 V at 450 ^{o}C, about twice smaller than that of the cell with Ag electrode. The high electrode/electrolyte interfacial polarization resistance may inevitably reduce the proton conduction. This could be interpreted by the low catalytic activity of Ag toward H_2 redox reaction [57] and the limited electrochemical reaction active sites - triple phase boundaries. The total polarization time of proton transport with Ag electrode, 40 min, is also much longer than that of the cell with reversible mixed metal oxide/electrolyte electrode (10 min) due to reduced electrode-electrolyte interface polarizations.

3.2.2 Oxygen ionic conductivity

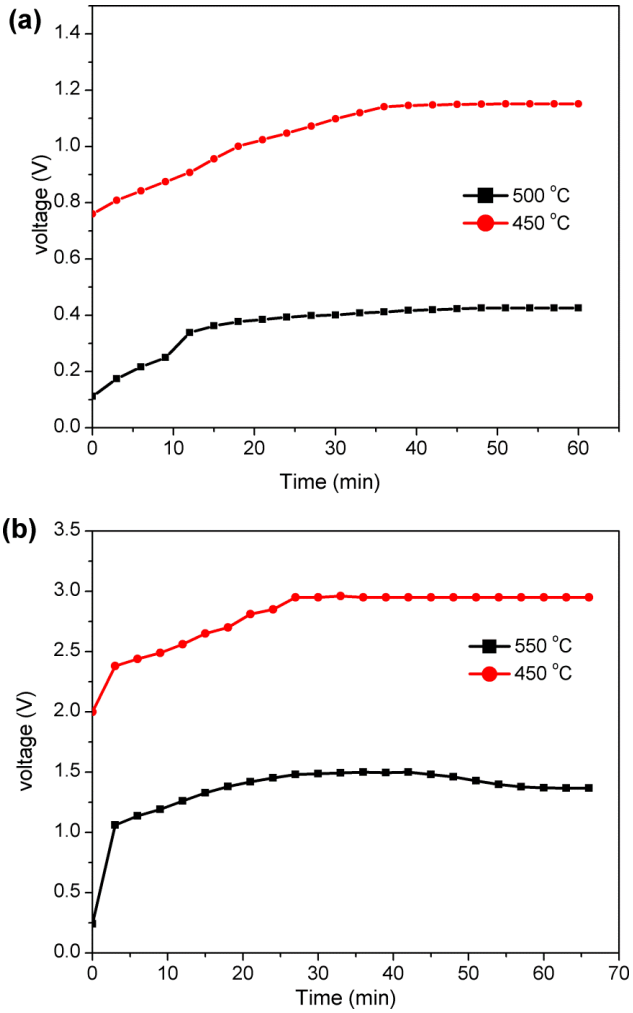

Figure 4. The polarization curve of electrolyte pellets under O_2 and 0.1 A constant DC current. (a) cell A and (b)

The oxygen ionic polarization process is shown in Fig. 4. Interestingly, only two-stage without voltage descending process is observed, which is visibly different from that of proton polarization at

the same conditions. This could be related with the intrinsic ionic conduction of SDCLN composite electrolyte [13].

Dislike proton introduced by the in-situ gas atmosphere, the oxygen ion transport inherent contributes to the total ionic conduction in the SDCLN. The DC oxygen ionic conductivity also increases with the applied temperature. However, when compared with the DC proton transport in SDCLN composite, much higher voltages are required for both cell A and cell B. For example, the applied voltage is 1.17 V for the constant oxygen ionic transport with reversible electrode at 450 ^{o}C, while it is only 0.38 V for steady state proton conduction at the same temperature. Therefore, the oxygen ionic conductivity is 2.07 times lower than conductivity of H^{+}, see Fig. 3. The ionic conduction phenomenon is consistent with the results reported by Wang [30] with similar material system. According to the above results, the ionic polarization process in SDC-carbonate composite is suggested as Fig. 5.

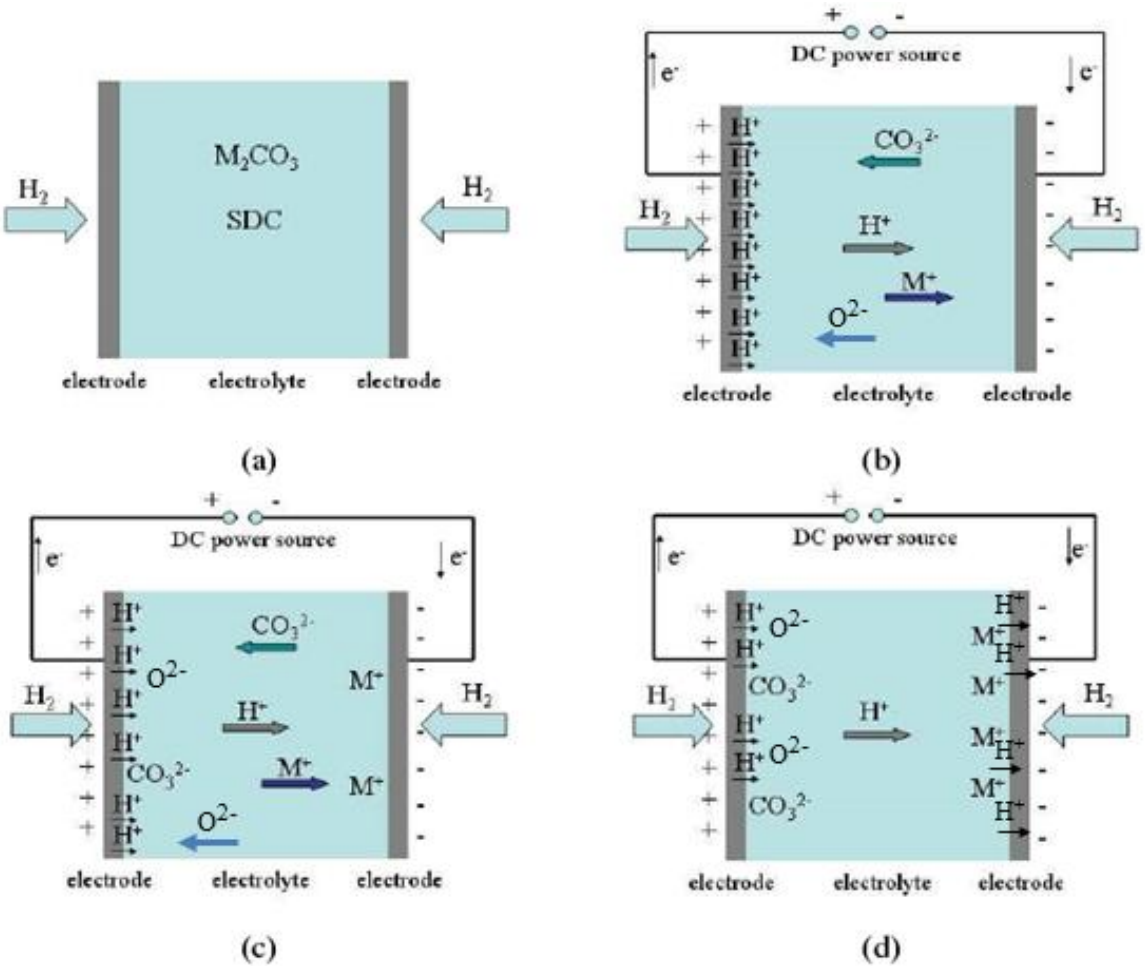

Figure 5. Scheme for multi-ionic polarization process in composite electrolyte during Wagner DC polarization. a) initial step without external potential, b) the first-step with external electrical field (0.1A constant density), c) second-step with double capacitor and continue proton transport and d) final steady state proton transfer in composite electrolyte [59]

Taking the proton conduction as an example, when there is no applied voltage between two electrodes in H_2 atmosphere, the multi-ions are homogeneous dispersed in the composite materials as

shown in Fig. 5a. The proton will gather first at the anode/electrolyte interface as soon as the voltage is employed, while other ions will start to move correspondingly in this electrical field, i.e. the carbonate ion and oxygen ion will move to anode while Na^+ and Li^+ will go to the cathode (Fig. 5b). With the constant applied voltage, the proton will gradually transfer to the cathode, but it needs some time to reach the interface of the cathode/ electrolyte, the same as other ions. The formed "electrical double layer" [58] by non-source ions causes the voltage rising in order to maintain the constant current flow. However, because of the non-source ionic nature, the voltage will not continuously increase; it will reach a peak value, as shown in Fig. 3 and Fig. 4. With the increase of time, the proton finally achieves the cathode/electrolyte interface. The interfacial activation will also promote the proton transfer and reduce the applied voltage. Finally, the proton transport reaches the steady-state as shown in the platform. For the oxygen ionic conduction, it is much easier compared to the proton transport. Therefore, there is only one voltage increase process due to the "electrical double layer" formation and the steady-state transport process.

Table 1. Calculation data of electrolyte conductivities (unit, S cm^{-1})

	Cell A		Cell B	
	550 ^oC	450 ^oC	550 ^oC	450 ^oC
$\sigma_{H+, DC}$	0.040	0.021	0.038	0.027
$\sigma_{O2-, DC}$	0.0184	0.0068	0.017	0.0079
$\sigma_{i-v, t}$	0.153	-	-	-

The ionic conductivity data calculated by the Wagner polarization and derived by fuel cell I-V curves are summarized in Table 1. As can be seen, the proton conductivities are higher than the oxygen ionic conductivities both for reversible electrode and Ag electrode. And pellet with reversible electrodes exhibits higher ionic conductivity than the un-reversible electrode. One may also see that the differences between proton and oxygen ionic conductivity increase with the decrease of the temperature. For instance, proton conductivity of the cell A is 1.2 times higher than that oxygen ionic conductivity at 550 ^oC (0.04 vs. 0.018 S cm^{-1}), which is increased to 2.1 when the temperature is reduced to 450 ^oC. It is well known that the proton conduction is much easier than oxygen conduction at low temperature. This is why the LTSOFC based on proton conductor attracts growing attention because the low temperature operation will significantly reduce the cost and improve the reliability of the high efficiency system. In addition, the oxygen conductivities at those temperatures are much higher than the widely used single phase electrolyte materials, such as SDC (600 ^oC, 0.01 S cm^{-1}) and YSZ (800 ^oC, 0.01 S cm^{-1}) [44], indicating that the O^{2-} with significantly high capacity is realized in such a composite system. There are two possible reasons for the enhanced oxygen ionic conductivity. One is that the high distorted SDC/carbonate interface providing a higher mobile ion concentration and a longer successive transport paths for the oxygen ionic transport [60]. The other one is that the existing of second phase of carbonates leads to the accumulation of oxygen ions n at the surface of an SDC particle, and thus resulting in a higher oxygen vacancy concentration in the SDC bulk due to the interfacial interaction [61].

One may observe that the DC conductivity derived from the fuel cell study is evidently higher than the sum of the proton and oxygen ion conductivity by Wagner polarization measurement in the tested temperature range. For instance, cell A shows a total ionic conductivity of 0.153 S cm^{-1}, 1.62 higher in fuel cell testing at 550 ^{o}C. The similar ionic conduction improvements are also observed between O^{2-}, CO_3^{2-} and other ionic in doped ceria-carbonate composites [9,11,26,32,62]. Wade et al. [26] found that a higher CO_2 permeability and selectivity of 6×10^{-12} mol m^{-1} s^{-1} Pa^{-1} was reached when doped ceria and tertiary carbonates composite was used compared with alumina-tertiary carbonates composite. Li et al. [9,11,62] showed that the electrochemical performance of fuel cell with doped ceria-carbonate electrolyte can be significantly improved when the cathode gas was switched from O_2 to O_2/CO_2 mixture. They suggested that the O^{2-} conductivity within ceria-carbonate composite could be effectively promoted by CO_3^{2-} ion migration. Furthermore, a recent interesting study funded by the Seventh Framework Programme of the European Commission (EP7) demonstrated a novel structural cell named "Ideal cell"[63,64,65]. In their experiments, water was formed within a porous mixed oxygen ion and proton conductive layer sandwiched by two respective dense oxygen ionic and protonic conductive membranes. This verifies that the oxygen ion and proton meet each other in the porous mixed conductive layer and produce water. In our previous work, we also have presented that the improved ionic conductivity of $BaCe_{0.8}Y_{0.2}O_{3-\delta}$ and SDC composite was obtained compared to the each single compound [32]. A recent work by Benamira et al. [66] supposed a mixed hydroxide and carbonate phase in the doped ceria-carbonate to explain the enhanced ionic conductivity and the lower melting point. They suggested that the OH^- was form by the following chemical reaction:

$$H_2O + O^{2-} \rightarrow 2OH^-$$

While H_2O was from the oxidation reactions:

$$H_2 + CO_3^{2-} \rightarrow H_2O + CO_2 + 2e^-$$

$$H_2 + O^{2-} \rightarrow H_2O + 2e^-$$

In addition, the water can formed when H^+ and O^{2-} meet together as demonstrated by the "Ideal cell" [64,65]:

$$2H^+ + O^{2-} \rightarrow H_2O$$

Even though the formed H_2O may not be in the liquid form at such a high temperature, proton conduction may actually be promoted and occur through successive proton transfers along the network [67]. Therefore, we believe that a synergistic effect exists between different ionic species which causes the enhanced total conductivity in the composite electrolyte and many other related phenomena.

An interfacial model for the two-phase composites of SDC-carbonate is suggested, as shown in Fig. 6(a). It could depict the difference between the H^+ and O^{2-} transport in such a composite system. The carbonates (the green balls) coats around the SDC matrix (like those red, white, blue, yellow big

bulks), forming a nano-scale ion flow highways. The H^+ (the tiny red balls) conducts along the interface between SDC and carbonate, while O^{2-} (such as blue big balls) transports through the bulk SDC and also the interface. An SEM image of the composite electrolyte is also shown in Fig. 6(b). As can be seen from this figure, the nano-scale SDC powders were homogeneously surrounded by the carbonates. The large amount of contacts or interfaces between carbonate and SDC will provide a high-speed way for ionic migration in the composite electrolyte.

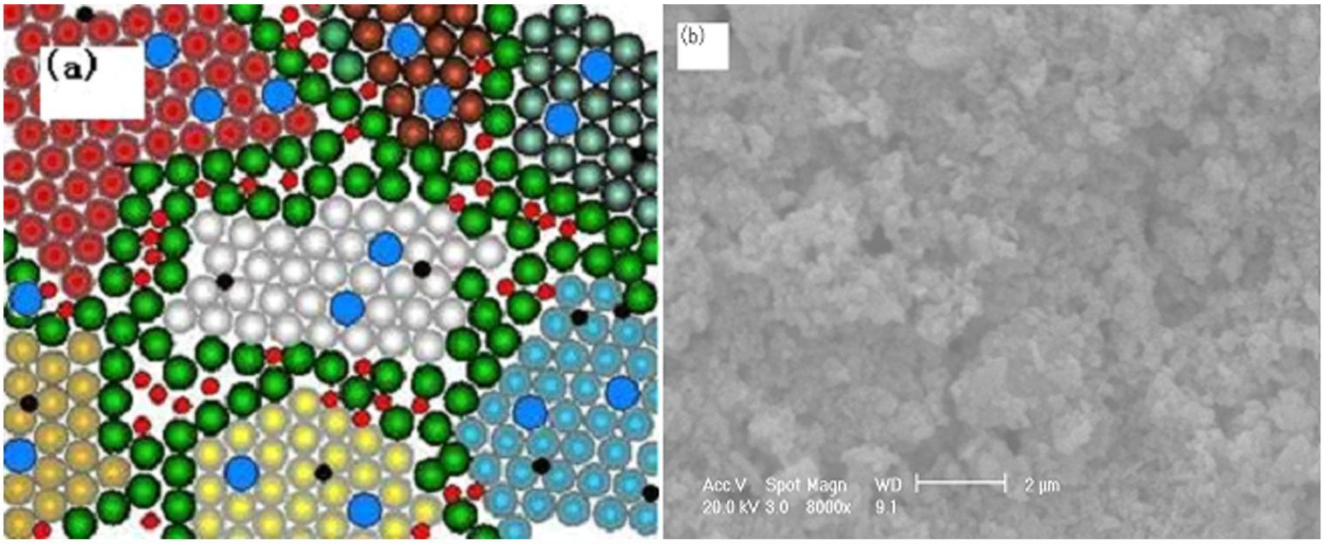

Figure 6. (a) A ideal interfacial conduction model of SDC-carbonate composite and (b) SEM micrograph of the SDC-carbonate electrolyte powders

3.3. The ion polarization time in multi-ion system

In the non-source ion and dielectric polarization process, Li^+, Na^+, CO_3^{2-} ions transported in the two-phase electrolyte/electrode interfaces and clusters interior under the electric field can be estimated. The Faraday electrolysis law can be used to calculate the maximal ion transport time [58], t:

$$t = mN_0eZ/AI$$

Where m is ionic species including Li^+, Na^+ and CO_3^{2-}, respectively; N_0 , the Avogadro's constant; e, unit negative electric charge (1.602×10^{-9} coulomb); Z, ionic valence; A, atomic weight and I is current.

They can be calculated based on the whole electrolyte including $LiNaCO_3$ ($2Li_2CO_3$: 1 Na_2CO_3 in molar ratio) of 20 %. For example, the weight of the composite electrolyte used in the measurements was among the 0.25 g to 0.3 g, where a 20 % weight is $LiNaCO_3$. We assume that all ions in these $LiNaCO_3$ contained ions can be transported. From the above equations, the maximal whole transport time of whole Li^+, Na^+, and CO_3^{2-} ions together can be calculated to be lower than 25 min. After the 25 min the stable transport plateau in the DC Polarization curves thus reflects certainly the source ions transport, as seen from Fig. 3 and Fig. 4.

4. CONCLUSIONS

In this study, conductive behaviors of open and multi-ionic and open system are sophisticated using doped ceria-carbonate composite as an example. New electrochemical analysis methodology - modified Waggner polarization is appealing. The ionic polarization process (both the source ions and blocked ions) is detailed analyzed. Thus we are able to specify contributions of each ion charger carrier in the SDCNL composite system, in which the proton conductivity in is much higher than that of oxygen ion. A synergistic effect between various ions is found and the interfacial conduction model is suggested to interpret the much improved ionic conductivity of doped-ceria - carbonate composite.

ACKNOWLEDGEMENTS

This work is supported by the EC FP6 NANOCOFC project (Contract No. 032308), Swedish Research Council (VR, Contract No. 621-2011-4983)/the Swedish agency for international cooperation development (Sida), Carl Tryggers Stiftelse for Vetenskap Forskning (CTS) and the Natural Science Foundation of Tianjin City (No. 12JCZDJC27000). Liangdong Fan appreciates the financial supports from the China Scholarship Council (CSC, file No. 2010625060) to study at Royal Institute of Technology (KTH) in Sweden.

References

1. B. Zhu, X. Yang, J. Xu, Z. Zhu, S. Ji, M. Sun and J. Sun, *J. Power Sources* 118 (2003) 47.
2. B. Zhu, *J. Power Sources* 114 (2003) 1.
3. J. Huang, L. Yang, R. Gao, Z. Mao and C. Wang, *Electrochem. Commun.* 8 (2006) 785.
4. B. Feng, C.Y. Wang and B. Zhu, Electrochem. Solid State Lett. 9 (2006) A80.
5. W. Zhu, C. Xia, D. Ding, X. Shi and G. Meng, *Mater. Res. Bull.* 41 (2006) 2057.
6. J. Huang, Z. Mao, Z. Liu and C. Wang, *Electrochem. Commun.* 9 (2007) 2601.
7. J. Huang, Z. Mao, Z. Liu and C. Wang, *J. Power Sources* 175 (2008) 238.
8. X. Wang, Y. Ma, R. Raza, M. Muhammed and B. Zhu, *Electrochem. Commun.* 10 (2008) 1617.
9. C. Xia, Y. Li, Y. Tian, Q. Liu, Y. Zhao, L. Jia and Y. Li, *J. Power Sources* 188 (2009) 156.
10. W. Liu, Y.Y. Liu, B. Li, T.D. Sparks, X. Wei and W. Pan, *Compos. Sci. Technol.* 70 (2010) 181.
11. C. Xia, Y. Li, Y. Tian, Q. Liu, Z. Wang, L. Jia, Y. Zhao and Y. Li, *J. Power Sources* 195 (2010) 3149.
12. J. Di, M. Chen, C. Wang, J. Zheng, L. Fan and B. Zhu, *J. Power Sources* 195 (2010) 4695.
13. A.S.V. Ferreira, C.M.C. Soares, F.M.H.L.R. Figueiredo and F.M.B. Marques, *Int. J. Hydrogen Energy* 36 (2011) 3704.
14. X. Li, G. Xiao and K. Huang, *J. Electrochem. Soc.* 158 (2011) B225.
15. L. Zhang, X. Li, S. Wang, K.G. Romito and K. Huang, *Electrochem. Commun.* 13 (2011) 554.
16. L. Fan, C. Wang, M. Chen, J. Di, J. Zheng and B. Zhu, *Int. J. Hydrogen Energy* 36 (2011) 9987.
17. M. Benamira, A. Ringuedé, V. Albin, R.N. Vannier, L. Hildebrandt, C. Lagergren and M. Cassir, *J. Power Sources* 196 (2011) 5546.
18. L. Fan, C. Wang, J. Di, M. Chen, J. Zheng and B. Zhu, J. Nanosci. Nanotechnol. 12 (2012) 4941.
19. Y. Xia, Y. Bai, X. Wu, D. Zhou, X. Liu and J. Meng, *Int. J. Hydrogen Energy* 36 (2011) 6840.
20. L. Fan, B. Zhu, M. Chen, C. Wang, R. Raza, H. Qin, X. Wang, X. Wang and Y. Ma, *J. Power Sources* 203 (2012) 65.

21. T. Ristoiu, T. Petrisor Jr, M. Gabor, S. Rada, F. Popa, L. Ciontea and T. Petrisor, *J. Alloys Compd.* 532 (2012) 109.
22. L. Fan, C. Wang and B. Zhu, *Nano Energy* 1 (2012) 631.
23. M. Chen, C. Wang, X. Niu, S. Zhao, J. Tang and B. Zhu, *Int. J. Hydrogen Energy* 35 (2010) 2732.
24. L. Jia, Y. Tian, Q. Liu, C. Xia, J. Yu, Z. Wang, Y. Zhao and Y. Li, *J. Power Sources* 195 (2010) 5581.
25. Y. Li, Z. Rui, C. Xia, M. Anderson and Y.S. Lin, *Catal. Today* 148 (2009) 303.
26. J.L. Wade, C. Lee, A.C. West and K.S. Lackner, *J. Membr. Sci.* 369 (2011) 20.
27. I.A. Amar, C.T.G. Petit, L. Zhang, R. Lan, P.J. Skabara and S. Tao, *Solid State Ionics* 201 (2011) 94.
28. J. Huang, Z. Mao, L. Yang and R. Peng, *Electrochem. Solid State Lett.* 8 (2005) A437.
29. A. Bodén, J. Di, C. Lagergren, G. Lindbergh and C.Y. Wang, *J. Power Sources* 172 (2007) 520.
30. X. Wang, Y. Ma, S. Li, A.-H. Kashyout, B. Zhu and M. Muhammed, *J. Power Sources* 196 (2011) 2754.
31. Y. Zhao, C. Xia, Y. Wang, Z. Xu and Y. Li, *Int. J. Hydrogen Energy* 37 (2012) 8556.
32. B. Zhu, X.R. Liu and T. Schober, *Electrochem. Commun.* 6 (2004) 378.
33. B. Zhu and M. Mat, *Int. J. Electrochem. Sci.* 1 (2006) 383.
34. M.H. Hebb, *The Journal of Chemical Physics* 20 (1952) 185.
35. C. Wagner, *Zeitschrift fuer Elektrochemie und Angewandte Physikalische Chemie* 60 (1956) 4.
36. J. Wagner and C. Wagner, *The Journal of Chemical Physics* 26 (1957) 1597.
37. L. Navarro, F. Marques and J. Frade, *J. Electrochem. Soc.* 144 (1997) 267.
38. B.C.H. Steele, *Solid State Ionics* 129 (2000) 95.
39. T. Shimonosono, Y. Hirata, Y. Ehira, S. Sameshima, T. Horita and H. Yokokawa, *Solid State Ionics* 174 (2004) 27.
40. C. Chatzichristodoulou and P.V. Hendriksen, *PCCP* 13 (2011) 21558.
41. Y. Xiong, K. Yamaji, T. Horita, N. Sakai and H. Yokokawa, *J. Electrochem. Soc.* 149 (2002) E450.
42. Y.-P. Xiong, H. Kishimoto, K. Yamaji, M. Yoshinaga, T. Horita, M.E. Brito and H. Yokokawa, *Solid State Ionics* 192 (2011) 476.
43. B. Zhu, *Electrochem. Commun.* 1 (1999) 242.
44. S.M. Haile, *Acta Mater.* 51 (2003) 5981.
45. T. Matsui, T. Kosaka, M. Inaba, A. Mineshige and Z. Ogumi, *Solid State Ionics* 176 (2005) 663.
46. K.D. Kreuer, *Solid State Ionics* 125 (1999) 285.
47. A. Demin and P. Tsiakaras, *Int. J. Hydrogen Energy* 26 (2001) 1103.
48. H. Matsumoto, Y. Kawasaki, N. Ito, M. Enoki and T. Ishihara, *Electrochem. Solid-State Lett.* 10 (2007) B77.
49. E. Fabbri, D. Pergolesi and E. Traversa, *Chem. Soc. Rev.* 39 (2010) 4355.
50. H. Iwahara, H. Uchida and K. Morimoto, *J. Electrochem. Soc.* 137 (1990) 462.
51. C. Zuo, S. Zha, M. Liu, M. Hatano and M. Uchiyama, *Adv. Mater.* 18 (2006) 3318.
52. S. Kim, U. Anselmi-Tamburini, H.J. Park, M. Martin and Z.A. Munir, *Adv. Mater.* 20 (2008) 556.
53. H.J. Avila-Paredes, E. Barrera-Calva, H.U. Anderson, R.A. De Souza, M. Martin, Z.A. Munir and S. Kim, *J. Mater. Chem.* 20 (2010) 6235.
54. H.J. Avila-Paredes, C.-T. Chen, S. Wang, R.A. De Souza, M. Martin, Z. Munir and S. Kim, *J. Mater. Chem.* 20 (2010) 10110.
55. T. Schober, *Electrochem. Solid State Lett.* 8 (2005) A199.
56. Z. Tang, Q. Lin, B. Mellander and B. Zhu, *Int. J. Hydrogen Energy* 35 (2010) 2970.
57. A. Cantos-Gómez, R. Ruiz-Bustos and J. van Duijn, *Fuel Cells* 11 (2011) 140.
58. B. Zhu, Intermediate Temperature Solid Ionic Conductors and Fuel Cells, Doctoral thesis, 1995, Chalmers University of Technology, Sweden.

59. J. Di, Novel CeO2 based electrolyte for low and intermediate temperature solid oxide fuel cells, Doctoral thesis, 2009, Tianjin university, Tianjin, China
60. B. Zhu, *Int. J. Energy Res.* 33 (2009) 1126.
61. J. Huang, Z. Gao and Z. Mao, *Int. J. Hydrogen Energy* 35 (2010) 4270.
62. Y. Zhao, C. Xia, Y. Wang, Z. Xu and Y. Li, *Int. J. Hydrogen Energy* 37 (2012) 8556.
63. Innovative Dual mEmbrAne fuel Cell: IDEAL Cell, http://www.ideal-cell.eu/content/index.php. The last time access: 19st, May, 2012.
64. A.S. Thorel, A. Chesnaud, M. Viviani, A. Barbucci, S. Presto, P. Piccardo, Z. Ilhan, D.E. Vladikova and Z. Stoynov, *ECS Trans.* 25 (2009) 753.
65. D. Vladikova, Z. Stoynov, G. Raikova, A. Thorel, A. Chesnaud, J. Abreu, M. Viviani, A. Barbucci, S. Presto and P. Carpanese, *Electrochim. Acta* 56 (2011) 7955.
66. M. Benamira, A. Ringuedé, L. Hildebrandt, C. Lagergren, R.N. Vannier and M. Cassir, *Int. J. Hydrogen Energy* (2011) DOI: 10.1016/j.ijhydene.2011.10.062.
67. R. Vuilleumier and D. Borgis, *Nature Chemistry* 4 (2012) 432.